AGU PUBLICATIONS

Geophysical Research Letters

RESEARCH LETTER
10.1002/2016GL070107

Key Points:
- Highly improved database of earthquake focal mechanisms in the OBS lacking, mainly offshore seismic region of southern Italy
- Seismotectonic advances from the first application in southern Italy of a Bayesian stress inversion method
- Fine detection of seismogenic stress variation and local geodynamics along the plate margin segment of southern Italy

Supporting Information:
- Supporting Information S1
- Figure S1
- Table S1

Correspondence to:
C. Totaro,
ctotaro@unime.it

Citation:
Totaro, C., B. Orecchio, D. Presti, S. Scolaro, and G. Neri (2016), Seismogenic stress field estimation in the Calabrian Arc region (south Italy) from a Bayesian approach, *Geophys. Res. Lett.*, *43*, 8960–8969, doi:10.1002/2016GL070107.

Received 9 MAR 2016
Accepted 15 AUG 2016
Accepted article online 17 AUG 2016
Published online 7 SEP 2016

Seismogenic stress field estimation in the Calabrian Arc region (south Italy) from a Bayesian approach

C. Totaro[1], B. Orecchio[1], D. Presti[1], S. Scolaro[1], and G. Neri[1]

[1]Department of Mathematics, Computer Sciences, Physics, and Earth Sciences, University of Messina, Messina, Italy

Abstract A new high-quality waveform inversion focal mechanism database of the Calabrian Arc region has been compiled by integrating 292 mechanisms selected from literature and catalogs with 146 newly computed solutions. The new database has then been used for computation of posterior density distributions of stress tensor components by a Bayesian method never applied in south Italy before the present study. The application of this method to the enhanced database has allowed us to provide a detailed picture of seismotectonic stress regimes in this very complex area where lithospheric unit configuration and geodynamic engines are still strongly debated. Our results well constrain the extensional domain of Calabrian Arc and the compressional one of the southernmost Tyrrhenian Sea. In addition, previously undetected transcurrent regimes have been identified in the Ionian offshore. The new information released here will furnish useful tools and constraints for future geodynamic investigations.

1. Introduction

Seismic faulting is strictly related to tectonic stress acting in the lithosphere [*Dziewonski et al.*, 1981; *Anderson et al.*, 1993]. Various seismological methods and analyses for determining the components of tectonic stress tensor have been reported in the literature, and stress fields in many regions of the world are today known [see, e.g., *Heidbach et al.*, 2010]. Earthquake focal mechanisms are among the most used data for stress inversion (*McKenzie* [1969] and *Gephart and Forsyth* [1984], among many others). However, relatively low accuracy of focal mechanisms of older and/or lower magnitude earthquakes due in particular to limitations of seismic monitoring systems has prevented accurate stress estimates in many regions, and southern Italy is one of these.

In this paper we compiled a new database of shallow earthquake focal mechanisms relative to the Calabrian Arc region (Figure 1), a sector of great seismotectonic complexity [*Orecchio et al.*, 2014] that has been site of destructive earthquakes both in historical and more recent times [*Neri et al.*, 2006; *Galli et al.*, 2008]. The study region is particularly interesting because it is characterized by variable geodynamic settings and is the area where two of the main tectonic processes acting in the Mediterranean region, e.g., Africa-Eurasia convergence and the rollback of the Ionian subduction slab, coexist. In this region, different lithospheric units with changing thickness, composition, and kinematics have been detected (such as Ionian, Tyrrhenian, Sicily, and southern Apennines), even if the exact location of their boundaries, together with the effective roles of slow-rate Africa-Eurasia convergence and residual Ionian slab rollback on the regional geodynamics, are still matter of debate [*Devoti et al.*, 2008; *Pérouse et al.*, 2012; *Gallais et al.*, 2013; *Faccenna et al.*, 2014; *Carafa et al.*, 2015; *Polonia et al.*, 2016]. The new database has been compiled by adding 146 waveform inversion solutions estimated in this work to 292 selected from literature and official catalogs (see Table S1 in the supporting information for details). The inclusion of original solutions computed by the Cut And Paste (CAP) method [*Zhao and Helmberger*, 1994; *Zhu and Helmberger*, 1996] has permitted us to expand the existing set of data adding earthquakes of magnitude as small as 2.6 still keeping high quality of data [*D'Amico et al.*, 2010, 2011; *Orecchio et al.*, 2015].

Taking benefit from the enhanced set of focal mechanisms, we have investigated the seismogenic stress tensor variations over the study region. For this purpose, we have used a very effective Bayesian technique introduced for estimating tectonic stress parameters from primary seismological observations [*Arnold and Townend*, 2007] never applied in southern Italy before the present study. This technique allows to incorporate nodal plane ambiguity and observational errors in the computational process and furnishes the posterior density function for the principal components of stress tensor and the stress-magnitude ratio [*Townend et al.*, 2012]. The main aim of the present work is that of improving the knowledge of seismotectonic domains of Calabrian Arc and surrounding areas in south Italy.

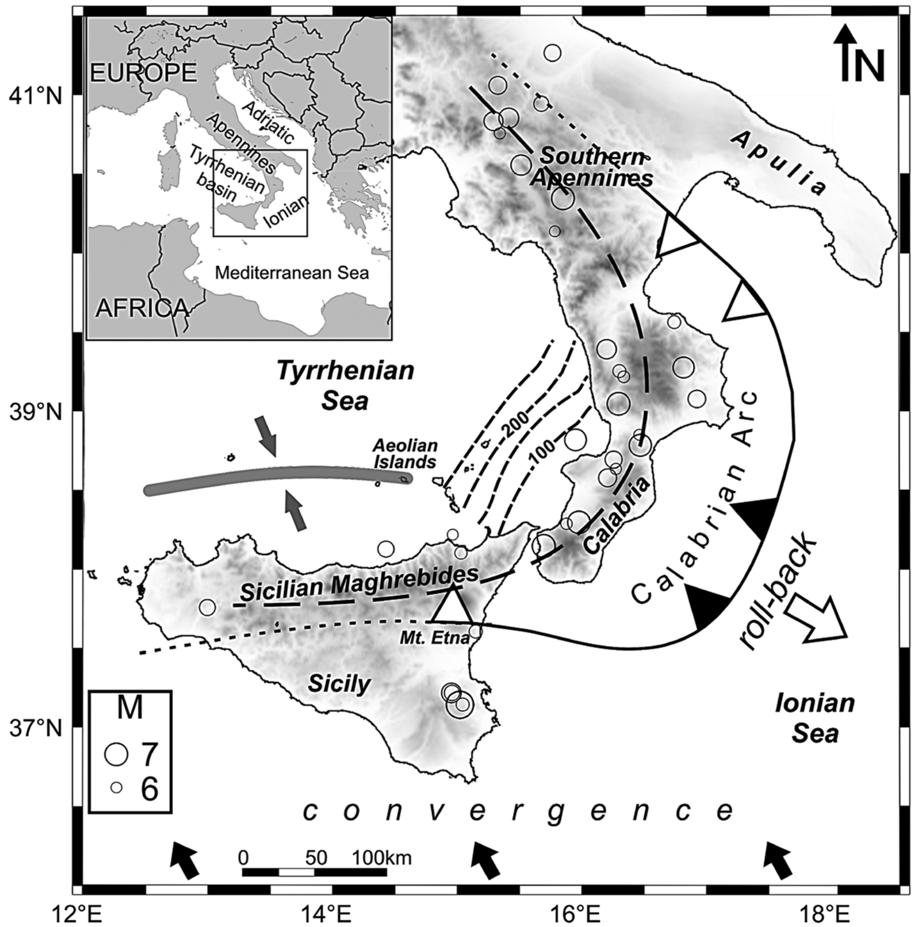

Figure 1. Map view of the study area. The solid curve with the sawtooth pattern, pointing in the direction of subduction, indicates the present-day location of the Ionian subducting system. According to recent literature (see, among others, *Neri et al.* [2009, 2012] and *Orecchio et al.* [2014]), black sawteeth indicate the continuous subducting slab while white sawteeth the plate boundary segments where slab has already undergone detachment. The white arrow shows the sense of the subducting slab rollback. The black arrows indicate the present motion of Africa relative to Europe [*Nocquet*, 2012, and references therein]. The large dashed curve running from Southern Apennines to Sicilian Maghrebides through Calabria indicates the Apennine-Maghrebian chain. West of the Aeolian Islands in the Tyrrhenian Sea, the grey belt indicates the location of the compressive margin accommodating the Africa-Eurasia convergence [*Billi et al.*, 2007, 2011; *Mastrolembo Ventura et al.*, 2014]. Circles show the locations of the earthquakes of magnitude 6.0 and larger that have occurred after 1000 A.D., according to the CPTI11 catalog [*Rovida et al.*, 2011; http://emidius.mi.ingv.it/CPTI11]. Thick dashed lines are depth contour lines of the Wadati-Benioff zone [*Faccenna et al.*, 2011]. In the upper right inset we report the study area (black box) in the wider regional framework.

2. Geodynamic Settings

The Calabrian Arc is a Cenozoic-Quaternary curved orogen corresponding to the sector of maximum curvature of the Apennine-Maghrebian chain in the central Mediterranean (Figure 1), which extends from the northern edge of Calabria to northeastern Sicily and represents a major tectonic structure in southern Italy [*Malinverno and Ryan*, 1986; *Rosenbaum and Lister*, 2004]. It shows a high level of heterogeneity in terms of seismotectonics and geodynamics [*Orecchio et al.*, 2014; *Palano*, 2015] and has been struck by up to magnitude 7 earthquakes both in historical and more recent times [*Neri et al.*, 2006; *Galli et al.*, 2008]. This structure originated in response to the Neogene-Quaternary convergence between Africa and Eurasia and rollback of the Ionian slab in the Central Mediterranean [*Malinverno and Ryan*, 1986; *Faccenna et al.*, 2004; *Rosenbaum and Lister*, 2004; *Billi et al.*, 2011; *Carminati et al.*, 2012]. It has experienced uplift process of 0.5–1.2 mm/yr in the last 1–0.7 Myrs, and normal faulting primarily accommodates its inner deformations [see, e.g., *Monaco and Tortorici*, 2000; *Neri et al.*, 2003]. As suggested by many workers (see, among others, *Malinverno and Ryan* [1986], *Neri et al.* [2005], and *Billi et al.* [2010]), different kinds of data available in this region can be framed in a geodynamic model presuming the coexistence of (i) NW-SE convergence of Africa and Eurasia plates currently accommodated along an ~E-W compressional belt located in the southern Tyrrhenian and (ii) southeastward rollback of the Ionian lithospheric slab subducting to northwest beneath the Tyrrhenian lithosphere (Figure 1). Plate convergence rate has been evaluated to be currently ~5 mm/yr [see *Nocquet*, 2012; *Palano et al*., 2012], while subduction trench retreat has been progressively decreasing in the last million years until reaching at present time values as small as 2 mm/yr [e.g., *D'Agostino et al*., 2011]. The very slow trench retreat of the remnant subducting slab inside a continental plate advancing slightly faster toward northwest probably led to a nonuniform advancement of the Ionian lithosphere margin [*Palano et al*., 2015].

Space-time evolution of the rollback process, that since Upper Pliocene appeared mainly confined in the Calabrian Arc area, can be referred to progressive variation of lithosphere that approaches the retreating trench. In particular, remarkable structural differences characterize the Ionian tectonic unit and the bordering ones of Sicily and Southern Apennines [*Catalano et al*., 2001; *Lucente and Speranza*, 2001; *Barberi et al*., 2004; *Orecchio et al*., 2011; *Totaro et al*., 2014]. Several geodynamic features of the study region (such as microplate boundaries and kinematics) are still uncertain [see, e.g., *Jenny et al*., 2006; *Nocquet*, 2012].

3. Data and Methods

An updated high-quality database of 438 crustal earthquake focal solutions has been compiled by taking from literature and catalogs the highest-quality waveform inversion solutions and adding 146 solutions computed in the present study (Figure 2).

Since it is widely accepted that waveform inversion focal solutions in the study area are much better constrained than *P* onset polarity ones (see, among others, *Pondrelli et al*. [2006], *Scognamiglio et al*. [2009], and *Presti et al*. [2013]), all the focal mechanisms selected in the present work are waveform inversion solutions (i) computed by the CAP method or (ii) coming from Italian centroid moment tensor (CMT), Regional CMT, and time domain moment tensor catalogs (http://www.ingv.it) [*Pondrelli et al*., 2006, 2011]. Focal mechanisms estimated by CAP are for earthquakes of magnitude $M \geq 2.6$ that originated at depths shallower than 40 km in the study region between January 2006 and October 2015 (Figure 2). In the CAP method [*Zhao and Helmberger*, 1994; *Zhu and Helmberger*, 1996], each waveform is broken up into Pnl (Pn followed by train of crust-trapped reflected/converted *P*-SV) and surface wave segments, which are given different weights during inversion. The same frequency bands have been used to filter synthetic and observed ground velocities, in detail 0.02–0.1 Hz for surface waves and 0.05–0.3 Hz for Pnl waves. Following previous investigations carried out in the study region [see, e.g., *D'Amico et al*., 2010, 2011; *Presti et al*., 2013; *Orecchio et al*., 2015], the robustness of CAP in our applications has been verified through rigorous tests in which recording network configuration, velocity, focal depth, and epicenter location are varied.

Formal errors on focal mechanism parameters (strike, dip, and rake) that we estimated during the inversion procedure using linearized algorithms (see *Tan et al*. [2006] for details) were of the order of 4°–5°. Error estimates from linear inversion methods tend, however, to be unrealistically small [see, e.g., *Presti et al*., 2008, and references therein], thus we performed additional tests. Following the approach by *Stich et al*. [2003], we constructed for each earthquake a set of “artificial” focal mechanisms moving in all directions around the focal mechanism solution in the focal parameter space. Then, we estimated the observed-versus-synthetic waveform RMS for all artificial focal mechanisms and compared these values with the RMS relative to the solution. Following *Stich et al*. [2003], we assumed that the uncertainty volume of the solution includes all the artificial focal mechanisms having RMS < 10% above the one of the solution. By application of this procedure to the solutions estimated by CAP in the present study, we found that uncertainties of focal mechanisms of our data set are of the order of 8°–10°. These solutions have been combined with the focal mechanisms selected from literature and official catalogs for earthquakes occurring at depth <40 km in southern Italy between 1977 and 2015 (Figure 2 and Table S1).

In order to estimate the stress distribution over the study region, this high-quality database has been used for stress tensor inversion by applying, for the first time in south Italy, the method by *Arnold and Townend* [2007]. These authors developed a Bayesian method for tectonic stress computation which furnishes the posterior density function of the principal components of stress tensor (maximum σ_1, intermediate σ_2, and minimum σ_3 compressive stress, respectively) and the stress-magnitude ratio (*R*). The parameter *R* is

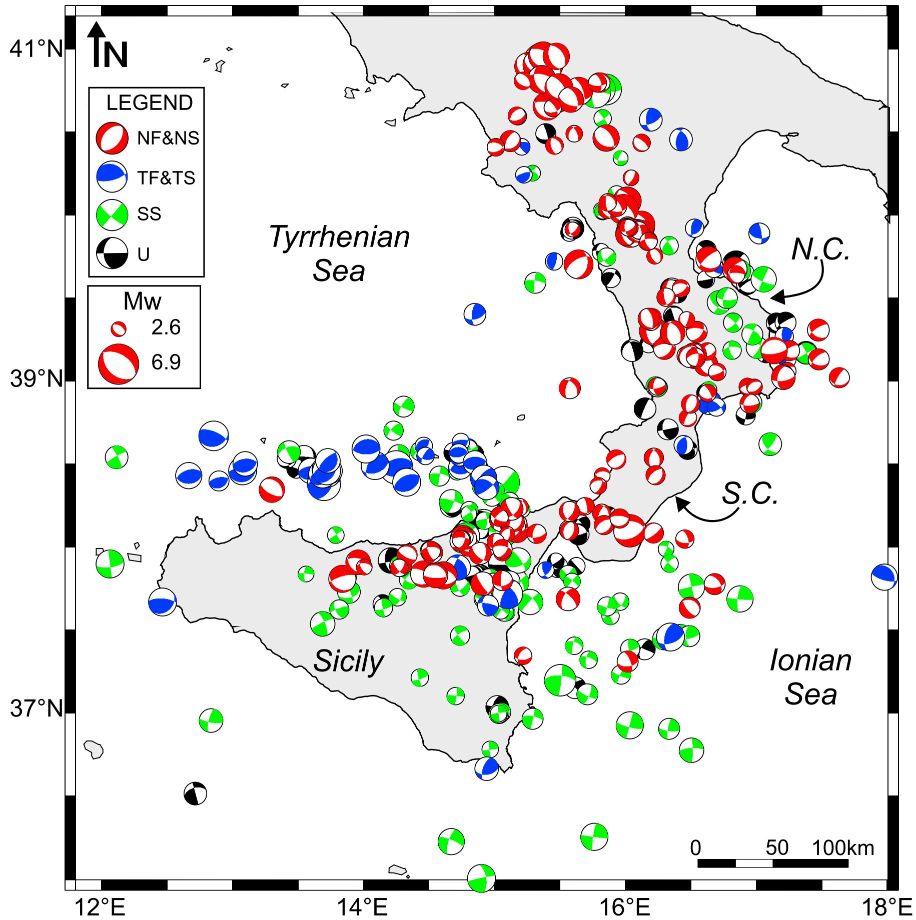

Figure 2. Database of crustal earthquake focal mechanisms for the study area. Different colors identify different types of mechanisms following *Zoback*'s [1992] classification based on values of plunges of *P* and *T* axes: red = normal faulting (NF) or normal faulting with a minor strike-slip component (NS); green = strike-slip faulting (SS); blue = thrust faulting (TF) or thrust faulting with a minor strike-slip component (TS); black = unknown stress regime (U). "U" includes all focal mechanisms which do not fall in the other five categories [*Zoback*, 1992]. The beach ball size is proportional to the earthquake magnitude (see legend). "N.C." and "S.C." stand for Northern Calabria and Southern Calabria, respectively.

used to determine the axis of maximum horizontal compressive stress (S_{Hmax}). Each focal mechanism is characterized by four parameters: strike, dip, rake, and a weight factor or precision τ. The τ value estimate is based on the assumption that fault parameter errors follow a Matrix-Fisher distribution (see, for more details, *Arnold and Townend* [2007] and *Mazzotti and Townend* [2010]). This Bayesian approach enables to incorporate nodal plane ambiguity, focal mechanism uncertainties, and similarity of the focal mechanisms included in each seismic zone [*Arnold and Townend*, 2007]. The latter criterion is important because additional similar solutions add little to the constraints on the stress than is provided by a single solution [*McKenzie*, 1969; *Hardebeck*, 2006; *Townend et al*., 2012]. Some of the most common algorithms for stress computation [see, e.g., *Gephart and Forsyth*, 1984] tend to be misleading in this regard [*Hardebeck and Michael*, 2004; *Townend*, 2006].

Before starting with stress computations, we applied the *k*-means nonhierarchical clustering algorithm [see, e.g., *Hartigan*, 1975] to subdivide the focal mechanism data set according to hypocentral locations. This algorithm is not guaranteed to furnish a globally optimal, or even unique, solution, but by fixing the number of clusters "*k*," it assures that each event is closer to the centroid of the cluster to which it is assigned than to the ones of all *k*-1 other clusters. It has already been applied by other investigators to focal mechanism data specifically [see, e.g., *Holt et al*., 2013]. Since clustering obtained by the *k*-means algorithm is based only on earthquake locations and not on faulting type, this approach allows identifying the sectors to be investigated without any "a priori" constraint from focal mechanism distribution.

For our data set we have tested several values of k and run the k-means algorithm 1000 times randomly selecting various starting points for each k. At last, we have chosen $k = 12$ which appeared the most appropriate number of clusters for our data set according to the "elbow criterion" based on analysis of data variance versus k [*Thorndike*, 1953]. We therefore report in Figure 3 the results obtained by using $k = 12$ clusters: the clusters contain on average 37 focal solutions and a minimum of 20, with the only exception of two clusters containing, respectively, 15 and 5 focal solutions (boxes 7 and 12 in Figure 3). For each cluster the stereonet reporting the contours of the σ_1, σ_2, and σ_3 axes at the 90% confidence level is shown (Figure 3b). The confidence areas of obtained stress fields appear, in general, quite concentrated, indicating a high level of resolution in most cases (see Figure S1 in the supporting information for more details). Additional inversion runs have been performed by partitioning each cluster according to earthquake magnitude or focal depth, in order to identify (i) eventual local effects of stress recognizable by low-magnitude earthquakes or (ii) stress changes between different tectonic domains distinguishable by depth. No change of stress as function of magnitude or depth has been detected.

4. Discussion of Results

In the recent literature different kinds of data and methods have been used in order to depict the present-day crustal stress in southern Italy [*Musumeci et al*., 2014; *Palano*, 2015; *Montone and Mariucci*, 2016]. *Musumeci et al*. [2014] and *Palano* [2015] have focused their attention on specific sectors of our study region and used focal solution data sets where lower quality P onset polarity solutions are dominant with respect to poor numbers of better quality waveform inversion ones. *Montone and Mariucci* [2016] have used a data set mainly consisting of CMT waveform inversion solutions, but the number of solutions available to them in our study region (slightly more than a hundred) has not permitted to detect more than the gross features of the regional stress, such as extension in the Apennine-Calabria region and compression in the northern offshore of Sicily. More accurate detection of stress tensor variations in the region including the Apennine-Maghrebian chain from south Italy to western Sicily and the Tyrrhenian and Ionian offshores has, conversely, been possible in the present study by means of inversion of a high-quality robust data set including 438 waveform inversion focal solutions.

Earthquake focal mechanisms and stress tensor distributions obtained in the present study (Figures 2 and 3) clearly indicate tectonic domains and suggest geodynamic engines. With their good level of constraint witnessed by posterior density errors as low as 5°–15° (Figures 3b and S1) our results clarify the stress patterns along the Apennine-Maghrebian chain and also allow improving the knowledge of stress regimes in the forearc area of the Ionian subduction zone, a sector not adequately investigated to date. The extensional dynamics and their changes along the Apennine-Maghrebian arcuate chain, where the Calabrian Arc roughly corresponds to the sector of maximum curvature, are well depicted by our results from the southern Apennines to western Sicily (Figure 4). Normal faulting solutions are mainly concentrated along the chain (Figures 2 and 1) and the opening direction detected by stress inversion is more or less perpendicular to the chain and follows with some approximation its curvature (boxes 1, 2, 4, 5, 8, and 10 in Figures 3 and 4). The Southern Apennines sector (Figure 2 and boxes 1 and 2 in Figure 3), which shows a predominance of normal faulting solutions leading to a steep σ_1 together with a horizontal NE trending σ_3, is presently undergoing extension probably related to postorogenic collapse tectonics [*Catalano et al*., 2004; *Barchi et al*., 2007; *Li et al*., 2007; *Reitz and Seeber*, 2012; *Totaro et al*., 2013, 2015]. The extensional regime of Calabria and Messina Straits area (Figure 2 and boxes 4, 5, and 8 in Figure 3) highlighted by high concentration of normal faulting solutions and stress patterns showing vertical σ_1 and horizontal SE trending σ_3, can be ascribed to southeastward rollback of the Ionian subducting slab [*Neri et al*., 2005; *D'Agostino et al*., 2011; *Presti et al*., 2013]. Looking in detail at the stress pattern of box 8, slight differences can be noted with respect to boxes 4 and 5. Box 8, in fact, is characterized by a σ_1 less steep than those detected for sectors 4 and 5. This reflects a mainly extensional stress pattern with a minor component of dextral strike-slip kinematics possibly due to local transition between collisional domains 9 and 11 and rollback-induced extension of sectors 4 and 5 [*Presti et al*., 2013; *Palano et al*., 2015].

The compressional tectonics active in the Southern Tyrrhenian Sea offshore Sicily is evidenced by predominance of thrust faulting leading to vertical σ_3 and ~NNW trending horizontal σ_1 (Figure 2 and boxes 9–11 in Figure 3) referable to Africa-Eurasia convergence in the central Mediterranean [*Pondrelli et al*., 2004; *Billi et al*., 2007, 2011; *Neri et al*., 2014]. We also obtained well-constrained stress fields in three large sectors located in

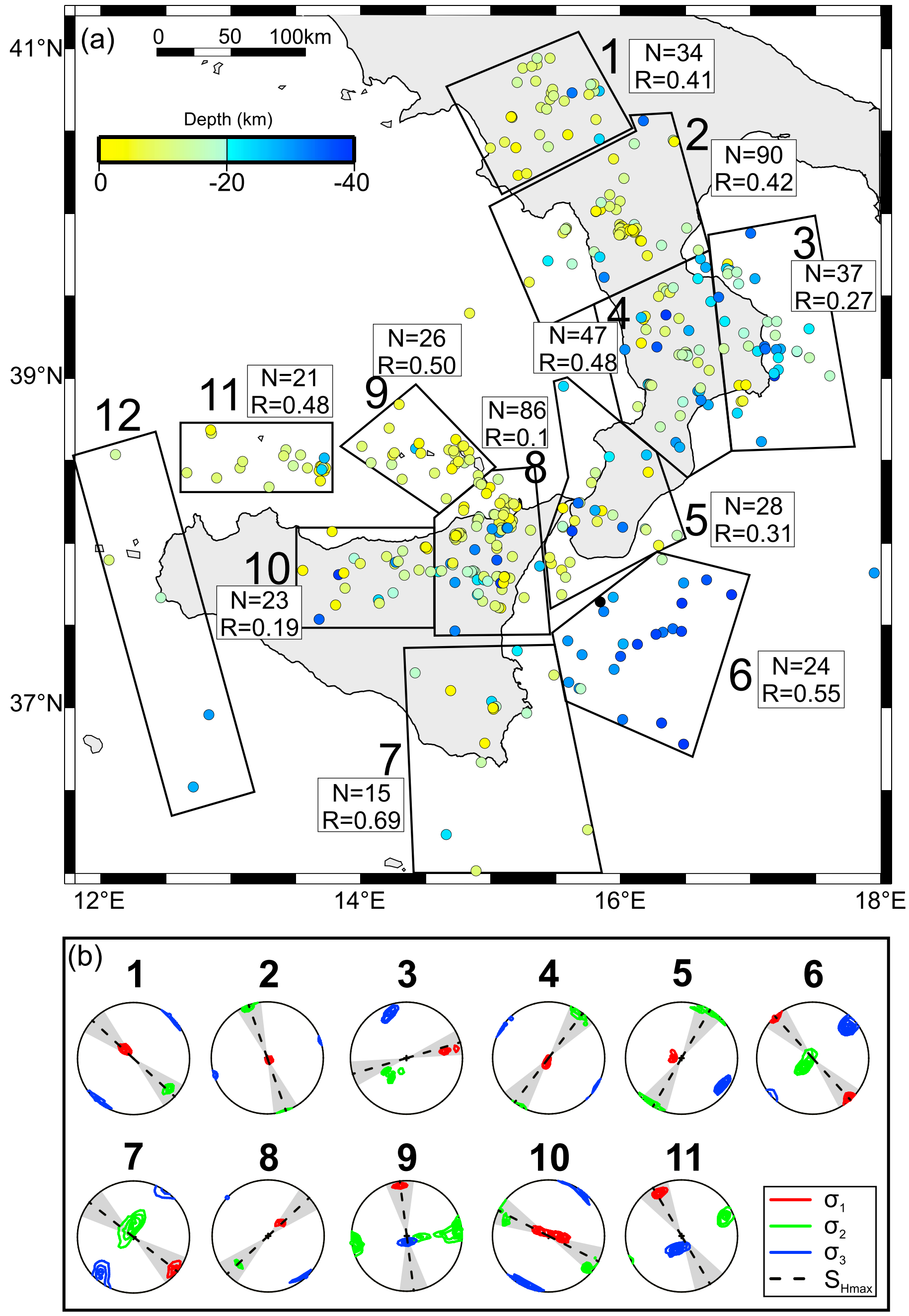

Figure 3. (a) Epicenters of the focal mechanisms shown in Figure 2 clustered by the *k*-means algorithm reported with a color code relative to focal depth. Numbers 1 to 12 indicate the clusters, *N* and *R* are the number of events and the stress-magnitude ratio relative to each cluster, respectively. (b) Stereonets showing the orientations of the principal stress axes estimated for each cluster (lower hemisphere projection; north is up, east is right). Red, green, and blue contours denote the positions of the σ_1, σ_2, and σ_3 axes, respectively, and the corresponding orientation of S_{Hmax} is marked as a black dashed line with the 90% confidence intervals shaded in gray. The numbers associate each stereonet to the relative cluster. The stereonet of cluster 12 is omitted because the low number of focal solutions available in the cluster (five) has not permitted to constrain the stress tensor.

the Ionian offshore of the study region (boxes 3, 6, and 7 in Figure 3) showing almost pure transcurrent regimes (Figure 4). In particular, the Ionian Calabria sector (box 3) is characterized by strike-slip solutions indicating left-lateral kinematics with NNW trending horizontal σ_3 and ENE trending subhorizontal σ_1 implying a minor extensional component. The obtained stress field probably reflects the transition between the area

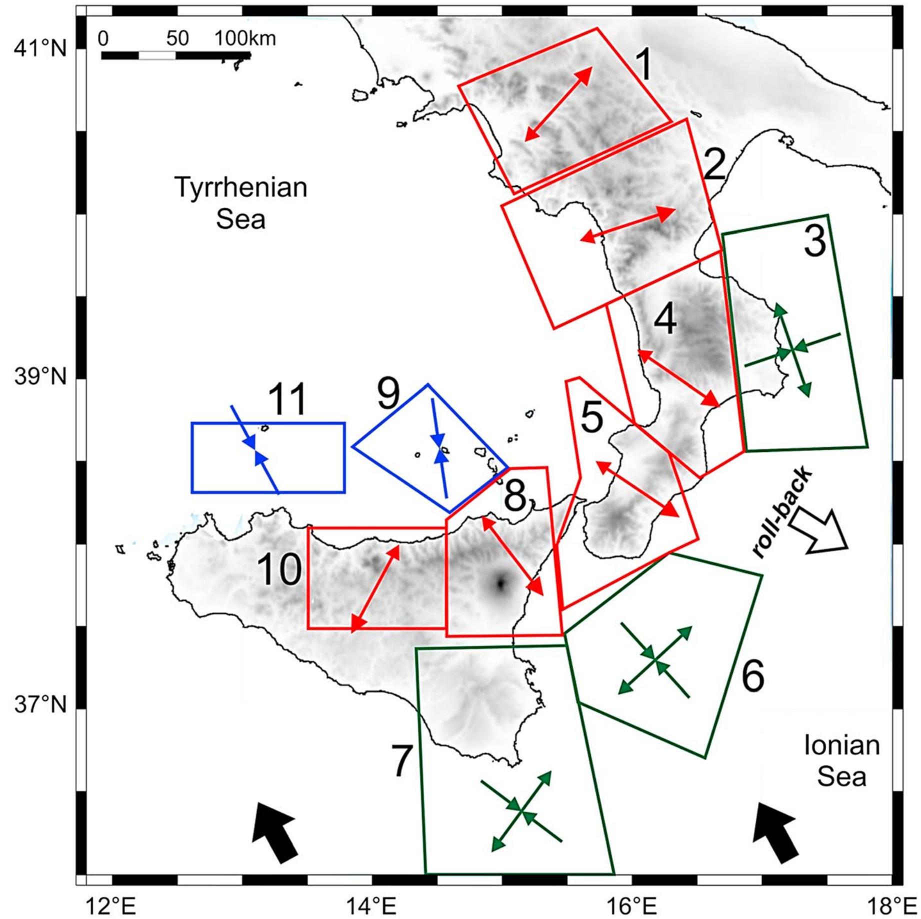

Figure 4. Synthesis of the stress orientations estimated in the present study for the southern Italy region. Numbers 1 to 11 indicate the focal mechanism clusters. The main extensional domains are depicted by red boxes reporting the orientation of σ_3 (red arrows). The compressional ones are indicated by blue boxes showing the orientation of σ_1 (blue arrows). Transcurrent domains identified in the Ionian offshore of the study region are indicated by green boxes for which both σ_1 and σ_3 are reported (green arrows). Black arrows indicate the present motion of Africa relative to Europe [*Nocquet*, 2012, and references therein] and the white one shows the sense of the residual subducting slab rollback.

where southeastward rollback of the Ionian subducting slab is still active (south, Figure 4) and the area where the subduction slab has already undergone detachment (north) (see also *Neri et al*. [2012]). Strike-slip solutions are also predominant in boxes 6 and 7 in the Ionian offshore. The stress field computed in sector 6 shows horizontal NW trending σ_1 and NE trending σ_3, expression of a pure transcurrent regime which can be ascribed to Africa-Eurasia convergence that is found oriented NW-SE in this sector of the Mediterranean [*Nocquet*, 2012]. In the Hyblean region and its immediate offshore (box 7) strike-slip solutions are also predominant and the obtained stress field, very similar to the one derived for box 6, reflects again the NW-SE Africa-Eurasia convergence. It seems also reasonable to suppose that relatively low level of seismicity detectable in the Ionian offshore of southern Calabria (Figure 2) (see also *Orecchio et al*. [2014]) can be an effect of southeastward rollback of the subducting slab active in the same zone (Figure 4) which locally reduces the compressional stress due to NW oriented plate convergence.

Finally, at the westernmost corner of Sicily (box 12 in Figure 3), the five focal mechanisms available for inversion do not guarantee an acceptable estimate of stress tensor orientations and these are therefore omitted in Figure 3b and in Figure 4.

5. Conclusions

The compilation of an updated waveform inversion focal mechanism database and the application of the Bayesian stress inversion algorithm by *Arnold and Townend* [2007] have permitted us (i) to strongly improve the knowledge of seismotectonic stress regimes in the Calabrian Arc region and (ii) to start exploring seismogenic stress in the Ionian offshore, an area where many investigations have provided other geological and geophysical information. The obtained stress distribution covers with good accuracy the whole arcuate region corresponding to the Apennine-Maghrebian chain from south Italy to western Sicily and the relative Tyrrhenian and Ionian offshores (Figure 4). Our analysis highlights, in particular, a more or less perpendicular-to-chain extensional process along the chain, compressional effects of Africa-Eurasia slow convergence mainly detected in the Tyrrhenian and Ionian offshores, and NW-SE extension along the Calabrian Arc that jointly with seismicity distribution in the Ionian offshore of the Arc can be related to southeastward retreat of the Ionian subducting slab. More in detail, the well constrained NNW trending σ_1 in the main east trending seismogenic belt located offshore northern Sicily, and the quite diffused transcurrent regimes in southeastern Sicily and Ionian offshore driven by NW trending $\sigma_{1,}$ mark clearly continental plate convergence. At the same time, relatively low level of seismicity in the Ionian offshore of southern Calabria and the extension of Calabrian Arc parallel to southeastward rollback of the Ionian subduction slab, may reflect the superposition of a quite localized residual subduction process onto the continental-scale process of convergence.

Our results consisting of a strongly enhanced focal mechanism database and more accurate local-to-regional scale stress distributions throw new light on the kinematics and dynamics of this still widely debated region and furnish useful tools and constraints for future geodynamic investigations.

Acknowledgments
We are very grateful to the Editor Andrew V. Newman and to Leonardo Seeber, John Townend, and an anonymous reviewer for comments and suggestions that significantly improved the manuscript. We also want to thank Richard Arnold and John Townend for their availability providing us the code. Data to support this article were collected from the INGV and the University of Calabria databases. This study has also benefited from funding provided by Regione Sicilia POR 2007-2013 project 162 “Attività di sviluppo sperimentale finalizzata alla riduzione del rischio sismico nella Sicilia Orientale.

References

Anderson, H., T. Webb, and J. Jackson (1993), Focal mechanisms of large earthquakes in the south-island of New Zealand—Implications for the accommodation of Pacific-Australia plate motion, *Geophys. J. Int.*, *115*, 1032–1054, doi:10.1111/j.1365-246X.1993.tb01508.x.

Arnold, R., and J. Townend (2007), A Bayesian approach to estimating tectonic stress from seismological data, *Geophys. J. Int.*, *170*, 1336–1356.

Barberi, G., M. T. Cosentino, A. Gervasi, I. Guerra, G. Neri, and B. Orecchio (2004), Crustal seismic tomography in the Calabrian Arc region, south Italy, *Phys. Earth Planet. Inter.*, *147*, 297–314.

Barchi, M., A. Amato, G. Cippitelli, S. Merlini, and P. Montone (2007), Extensional tectonics and seismicity in the axial zone of the Southern Apennines, in *Results of the CROP Project, Sub-Project CROP 04 Southern Apeninnes*, *Ital. J. Geosci*., vol. 7, edited by A. Mazzotti, E. Patacca, and P. Scandone, pp. 47–56, Bollettino della Societa Geologica Italiana, Italy.

Billi, A., D. Presti, C. Faccenna, G. Neri, and B. Orecchio (2007), Seismotectonics of the Nubia plate compressive margin in the south-Tyrrhenian region, Italy: Clues for subduction inception, *J. Geophys. Res.*, *112*, B08302, doi:10.1029/2006JB004837.

Billi, A., D. Presti, B. Orecchio, C. Faccenna, and G. Neri (2010), Incipient extension along the active convergent margin of Nubia in Sicily, Italy: Cefalù–Etna seismic zone, *Tectonics*, *29*, TC4026, doi:10.1029/2009TC002559.

Billi, A., C. Faccenna, O. Bellier, L. Minelli, G. Neri, C. Piromallo, D. Presti, D. Scrocca, and E. Serpelloni (2011), Recent tectonic reorganization of the Nubia–Eurasia convergent boundary heading for the closure of the western Mediterranean, *Bull. Soc. Géol. Fr.*, *182*, 279–303.

Carafa, M., S. Barba, and P. Bird (2015), Neotectonics and long-term seismicity in Europe and the Mediterranean region, *J. Geophys. Res. Solid Earth*, *120*, 5311–5342, doi:10.1002/2014JB011751.

Carminati, E., M. Lustrino, and C. Doglioni (2012), Geodynamic evolution of the central and western Mediterranean: Tectonics vs. igneous petrology constraints, *Tectonophysics*, doi:10.1016/j.tecto.2012.01.026.

Catalano, R., C. Doglioni, and S. Merlini (2001), On the Mesozoic Ionian Basin, *Geophys. J. Int.*, *144*, 49–64.

Catalano, S., C. Monaco, L. Tortorici, W. Paltrinieri, and N. Steel (2004), Neogene-Quaternary tectonic evolution of the southern Apennines, *Tectonics*, *23*, TC2003, doi:10.1029/2003TC001512.

D'Amico, S., B. Orecchio, D. Presti, L. Zhu, R. B. Herrmann, and G. Neri (2010), Broadband waveform inversion of moderate earthquakes in the Messina Straits, southern Italy, *Phys. Earth Planet. Inter.*, *179*, 97–106.

D'Amico, S., B. Orecchio, D. Presti, A. Gervasi, L. Zhu, I. Guerra, G. Neri, and R. B. Herrmann (2011), Testing the stability of moment tensor solutions for small earthquakes in the Calabro-Peloritan Arc region (southern Italy), *Boll. Geofis. Teor. Appl.*, *52*(2), 283–298.

D'Agostino, N., E. D'Anastasio, A. Gervasi, I. Guerra, M. R. Nedimović, L. Seeber, and M. Steckler (2011), Forearc extension and slow rollback of the Calabria Arc from GPS measurements, *Geophys. Res. Lett.*, *38*, L17304, doi:10.1029/2011GL048270.

Devoti, R., F. Riguzzi, M. Cuffaro, and C. Doglioni (2008), New GPS constraints on the kinematics of the Apennines subduction, *Earth Planet. Sci. Lett.*, *273*, 163–174.

Dziewonski, A. M., T. A. Chou, and J. H. Woodhouse (1981), Determination of earthquake source parameters from waveform data for studies of global and regional seismicity, *J. Geophys. Res.*, *86*, 2825–2852, doi:10.1029/JB086iB04p02825.

Faccenna, C., C. Piromallo, A. Crespo-Blanc, and L. Jolivet (2004), Lateral slab deformation and the origin of the western Mediterranean arcs, *Tectonics*, *23*, TC1012, doi:10.1029/2002TC001488.

Faccenna, C., P. Molin, B. Orecchio, V. Olivetti, O. Bellier, F. Funiciello, L. Minelli, C. Piromallo, and A. Billi (2011), Topography of the Calabria subduction zone (southern Italy): Clues for the origin of Mt. Etna, *Tectonics*, *30*, TC1003, doi:10.1029/2010TC002694.

Faccenna, C., et al. (2014), Mantle dynamics in the Mediterranean, *Rev. Geophys.*, *52*, 283–332, doi:10.1002/2013RG000444.

Gallais, F., D. Graindorge, M. Gutscher, and D. Klaeschen (2013), Propagation of alithospheric tear fault (STEP) through the western boundary of the Calabrian accretionary wedge offshore eastern Sicily (Southern Italy), *Tectonophysics*, *602*, 141–152, doi:10.1016/j.tecto.2012.12.026.

Galli, P., F. Galadini, and D. Pantosti (2008), Twenty years of paleoseismology in Italy, *Earth Sci. Rev.*, *88*, 89–117.

Gephart, J., and W. Forsyth (1984), An improved method for determining the regional stress tensor using earthquake focal mechanism data: Application to the San Fernando earthquake sequence, *J. Geophys. Res.*, *89*, 9305–9320, doi:10.1029/JB089iB11p09305.

Hardebeck, J. (2006), Homogeneity of small-scale earthquake faulting, stress, and fault strength, *Bull. Seismol. Soc. Am.*, *96*, 1675–1688, doi:10.1785/0120050257.

Hardebeck, J. L., and A. J. Michael (2004), Stress orientations at intermediate angles to the San Andreas fault, California, *J. Geophys. Res.*, *109*, B11303, doi:10.1029/2004JB003239.

Hartigan, J. A. (1975), *Clustering Algorithms*, Wiley, New York.

Heidbach, O., M. Tingay, A. Barth, J. Reinecker, D. Kurfeß, and B. Muller (2010), Global crustal stress pattern based on the World Stress Map database release 2008, *Tectonophysics*, *482*(1–4), 3–15.

Holt, R. A., M. K. Savage, J. Townend, E. M. Syracuse, and C. H. Thurber (2013), Crustal stress and fault strength in the Canterbury Plains, New Zealand, *Earth Planet. Sci. Lett.*, *383*, 173–181.

Jenny, S., S. Goes, D. Giardini, and H. G. Kahle (2006), Seismic potential of southern Italy, *Tectonophysics*, *415*, 81–101.

Li, H., A. Michelini, L. Zhu, F. Bernardi, and M. Spada (2007), Crustal velocity structure in Italy from analysis of regional seismic waveforms, *Bull. Seismol. Soc. Am.*, *97*, 2024–2039, doi:10.1785/0120070071.

Lucente, F. P., and F. Speranza (2001), Belt bending driven by lateral bending of subducting lithospheric slab: Geophysical evidences from the northern Apennines (Italy), *Tectonophysics*, *337*(1), 53–64.

Malinverno, A., and W. Ryan (1986), Extension in the Tyrrhenian Sea and shortening in the Apennines as result of arc migration driven by sinking of the lithosphere, *Tectonics*, *5*, 227–245, doi:10.1029/TC005i002p00227.

Mastrolembo Ventura, B., E. Serpelloni, A. Argnani, A. Bonforte, R. Bürgmann, M. Anzidei, P. Baldi, and G. Puglisi (2014), Fast geodetic strain-rates in eastern Sicily (southern Italy): New insights into block tectonics and seismic potential in the area of the great 1693 earthquake, *Earth Planet. Sci. Lett.*, *404*, 77–88, doi:10.1016/j.epsl.2014.07.025.

Mazzotti, S., and J. Townend (2010), State of stress in central and eastern North American seismic zones, *Lithosphere*, *2*(2), 776–83.

McKenzie, D. (1969), The relationship between fault plane solutions for earthquakes and the directions of the principal stresses, *Bull. Seismol. Soc. Am.*, *59*, 591–601.

Monaco, C., and L. Tortorici (2000), Active faulting in the Calabrian arc and eastern Sicily, *J. Geodyn.*, *29*, 407–424.

Montone, P., and M. T. Mariucci (2016), The new release of the Italian contemporary stress map, *Geophys. J. Int.*, *205*, 1525–1531.

Musumeci, C., L. Scarfì, M. Palano, and D. Patanè (2014), Foreland segmentation along an active convergent margin: New constraints in southeastern Sicily (Italy) from seismic and geodetic observations, *Tectonophysics*, *630*, 137–149, doi:10.1016/j.tecto.2014.05.017.

Neri, G., G. Barberi, B. Orecchio, and A. Mostaccio (2003), Seismic strain and seismogenic stress regimes in the crust of the southern Tyrrhenian region, *Earth Planet. Sci. Lett.*, *213*, 97–112.

Neri, G., G. Barberi, G. Oliva, and B. Orecchio (2005), Spatial variations of seismogenic stress orientations in Sicily, south Italy, *Phys. Earth Planet. Inter.*, *148*, 175–191.

Neri, G., G. Oliva, B. Orecchio, and D. Presti (2006), A possible seismic gap within a highly seismogenic belt crossing Calabria and eastern Sicily, Italy, *Bull. Seismol. Soc. Am.*, *96*(4A), 1321–1331, doi:10.1785/0120050170.

Neri, G., B. Orecchio, C. Totaro, G. Falcone, and D. Presti (2009), Seismic tomography says that lithospheric subduction beneath south Italy is close to die, *Seismol. Res. Lett.*, *80*, 63–70, doi:10.1785/gssrl.80.1.63.

Neri, G., A. M. Marotta, B. Orecchio, D. Presti, C. Totaro, R. Barzaghi, and A. Borghi (2012), How lithospheric subduction changes along the Calabrian Arc in southern Italy: Geophysical evidences, *Int. J. Earth Sci.*, *101*, 1949–1969.

Neri, G., M. Aloisi, F. Cannavò, B. Orecchio, M. Palano, D. Presti, G. Siligato, and C. Totaro (2014), Crustal stress and strain distribution in Sicily (Southern Italy) from joint analysis of seismicity and geodetic data AGU Fall Meeting, Abstract-ID: T33B-4691.

Nocquet, J. (2012), Present-day kinematics of the Mediterranean: A comprehensive overview of GPS results, *Tectonophysics*, *579*, 220–242.

Orecchio, B., D. Presti, C. Totaro, I. Guerra, and G. Neri (2011), Imaging the velocity structure of the Calabrian Arc region (South Italy) through the integration of different seismological data, *Boll. Geofis. Teor. Appl.*, *52*, 625–638.

Orecchio, B., D. Presti, C. Totaro, and G. Neri (2014), What earthquakes say concerning residual subduction and STEP dynamics in the Calabrian Arc region, south Italy, *Geophys. J. Int.*, *199*, 1929–1942, doi:10.1093/gji/ggu373.

Orecchio, B., D. Presti, C. Totaro, S. D'Amico, and G. Neri (2015), Investigating slab edge kinematics through seismological data: The northern boundary of the Ionian subduction system (south Italy), *J. Geodyn.*, *88*, 23–25, doi:10.1016/j.jog.2015.04.003.

Palano, M. (2015), On the present-day crustal stress, strain-rate fields and mantle anisotropy pattern of Italy, *Geophys. J. Int.*, *200*, 969–985, doi:10.1093/gji/ggu451.

Palano, M., L. Ferranti, C. Monaco, M. Mattia, M. Aloisi, V. Bruno, F. Cannavò, and G. Siligato (2012), GPS velocity and strain fields in Sicily and southern Calabria, Italy: Updated geodetic constraints on tectonic block interaction in the central Mediterranean, *J. Geophys. Res.*, *117*, B07401, doi:10.1029/2012JB009254.

Palano, M., D. Schiavone, M. Loddo, M. Neri, D. Presti, R. Quarto, C. Totaro, and G. Neri (2015), Active upper crust deformation pattern along the southern edge of the Tyrrhenian subduction zone (NE Sicily): Insights from a multidisciplinary approach, *Tectonophysics*, *657*, 205–218.

Pérouse, E., N. Chamot-Rooke, A. Rabaute, P. Briole, F. Jouanne, I. Georgiev, and D. Dimitrov (2012), Bridging onshore and offshore present-day kinematics of central and eastern Mediterranean: Implications for crustal dynamics and mantle flow, *Geochem. Geophys. Geosyst.*, *13*, Q09013, doi:10.1029/2012GC004289.

Polonia, A., et al. (2016), The Ionian and Alfeo-Etna fault zones: New segments of an evolving plate boundary in the central Mediterranean Sea?, *Tectonophysics*, *675*, 69–90.

Pondrelli, S., C. Piromallo, and E. Serpelloni (2004), Convergence vs. retreat in Southern Tyrrhenian Sea: Insights from kinematics, *Geophys. Res. Lett.*, *31*, L06611, doi:10.1029/2003GL019223.

Pondrelli, S., S. Salimbeni, G. Ekström, A. Morelli, P. Gasperini, and G. Vannucci (2006), The Italian CMT dataset from 1977 to the present, *Phys. Earth Planet. Int.*, *159*(3–4), 286–303, doi:10.1016/j.pepi.2006.07.008.

Pondrelli, S., S. Salimbeni, A. Morelli, G. Ekström, L. Postpischl, G. Vannucci, and E. Boschi (2011), European-Mediterranean regional centroid moment tensor catalog: Solutions for 2005–2008, *Phys. Earth Planet. Int.*, *185*(3), 74–81.

Presti, D., B. Orecchio, G. Falcone, and G. Neri (2008), Linear versus nonlinear earthquake location and seismogenic fault detection in the southern Tyrrhenian Sea, Italy, *Geophys. J. Int.*, *172*, 607–618.

Presti, D., A. Billi, B. Orecchio, C. Totaro, C. Faccenna, and G. Neri (2013), Earthquake focal mechanisms, seismogenic stress, and seismotectonics of the Calabrian Arc. Italy, *Tectonophysics*, *602*, 153–175, doi:10.1016/j.tecto.2013.01.030.

Reitz, M. A., and L. Seeber (2012), Arc-parallel strain in a short rollback subduction system: The structural evolution of the Crotone basin (northeastern Calabria, southern Italy), *Tectonics*, *31*, TC4017, doi:10.1029/2011TC003031.

Rosenbaum, G., and G. S. Lister (2004), Neogene and Quaternary rollback evolution of the Tyrrhenian sea, the Apennines, and the Sicilian Maghrebides, *Tectonics*, *23*, TC1013, doi:10.1029/2003TC001518.

Rovida, A., R. Camassi, P. Gasperini, and M. Stucchi (2011), *CPTI11, la versione 2011 del Catalogo Parametrico dei Terremoti Italiani*, Milano, Bologna. [Available at http://emidius.mi.ingv.it/CPTI.]

Scognamiglio, L., E. Tinti, and A. Michelini (2009), Real-time determination of seismic moment tensor for the Italian region, *Bull. Seismol. Soc. Am.*, *99*(4), 2223–2242, doi:10.1785/0120080104.

Stich, D., C. J. Ammon, and J. Morales (2003), Moment tensor solutions for small and moderate earthquakes in the Ibero-Maghreb region, *J. Geophys. Res.*, *108*(B3), 2148, doi:10.1029/2002JB002057.

Tan, Y., L. Zhu, D. Helmberger, and C. Saikia (2006), Locating and modeling regional earthquakes with two stations, *J. Geophys. Res.*, *111*, B01306, doi:10.1029/2005JB003775.

Thorndike, R. L. (1953), Who belongs in the family?, *Psychometrika*, *18*(4), 267–76.

Totaro, C., D. Presti, A. Billi, A. Gervasi, B. Orecchio, I. Guerra, and G. Neri (2013), The ongoing seismic sequence at the Pollino Mountains, Italy, *Seismol. Res. Lett.*, *84*(6), 955–962, doi:10.1785/0220120194.

Totaro, C., I. Koulakov, B. Orecchio, and D. Presti (2014), Detailed crustal structure in the area of the southern Apennines–Calabrian Arc border from local earthquake tomography, *J. Geodyn.*, *82*, 87–97, doi:10.1016/j.jog.2014.07.004.

Totaro, C., L. Seeber, F. Waldhauser, M. Steckler, A. Gervasi, I. Guerra, B. Orecchio, and D. Presti (2015), An intense earthquake swarm in the southernmost Apennines: Fault architecture from high-resolution hypocenters and focal mechanisms, *Bull. Seismol. Soc. Am.*, *105*(6), 3121–3128, doi:10.1785/0120150074.

Townend, J. (2006), What do faults feel? Observational constraints on the stress acting on seismogenic faults, in *Earthquakes: Radiated Energy and Physics of Faulting*, *Geophys. Monogr. Ser.*, vol. 170, edited by R. Abercrombie et al., pp. 313–327, AGU, Washington, D. C.

Townend, J., S. Sherburn, R. Arnold, C. Boese, and L. Woods (2012), Three-dimensional variations in present-day tectonic stress along the Australia–Pacific plate boundary in New Zealand, *Earth Planet. Sci. Lett.*, *353–354*, 47–59, doi:10.1016/j.epsl.2012.08.003.

Zhao, L. S., and D. Helmberger (1994), Source estimation from broad-band regional seismograms, *Bull. Seismol. Soc. Am.*, *85*, 590–605.

Zhu, L., and D. Helmberger (1996), Advancement in source estimation technique using broadband regional seismograms, *Bull. Seismol. Soc. Am.*, *86*, 1634–1641.

Zoback, M. L. (1992), First- and second-order patterns of stress in the lithosphere: The world stress map project, *J. Geophys. Res.*, *97*(B8), 11,703–11,728, doi:10.1029/92JB00132.